Hypothesis about electron quantum tunneling during sonochemical splitting of water molecule

Sergey I. Nikitenko, Timothé Di Pasquale, Tony Chave, Rachel Pflieger

Hypothesis about electron quantum tunneling during sonochemical splitting of water molecule

Sergey I. Nikitenko,* Timothé Di Pasquale, Tony Chave, Rachel Pflieger

Université de Montpellier, Institut de Chimie Séparative de Marcoule (ICSM), UMR 5257, CEA-CNRS-UM-ENSCM, Site de Marcoule BP17171, 30207 Bagnols sur Cèze, France

*To whom correspondence should be addressed. Email: serguei.nikitenko@cea.fr

Keywords: sonochemistry, kinetic isotope effect, quantum tunneling, water splitting, plasma

Abstract

Quantum tunneling in chemistry is often attributed to the processes at low or near room temperatures when the rate of thermal reactions becomes far less than the rate of quantum tunneling. However, in some rapid processes, quantum tunneling can be observed even at high temperatures. Herein, we report the experimental evidence for anomalous H/D kinetic isotope effect (KIE) during sonochemical dissociation of water molecule driven by 20 kHz power ultrasound measured in H_2O/D_2O mixtures saturated with Ar or Xe. Hydrogen released during ultrasonic treatment is enriched by light isotope. The observed H/D KIE (α=2.15-1.50) is much larger than what is calculated assuming a classical KIE for T_g=5000 K (α=1.15) obtained from the sonoluminescence spectra in H_2O and D_2O. Furthermore, the α values sharply decrease with increasing of H_2O content in H_2O/D_2O mixtures reaching a steady-state value close to α=1.50, which also cannot be explained by O-H/O-D zero-point energy difference. We suggest that these results can be understood in terms of quantum electron tunneling occurring in nonequilibrium picosecond plasma produced at the last stage of cavitation bubble collapse. Thermal homolytic splitting of water molecule is inhibited by extremely short lifetime of such plasma. On the contrary, immensely short traversal time for electron tunneling in water allows H_2O dissociation by quantum tunneling mechanism.

Discovered in 1929, the splitting of water under the effect of power ultrasound [1] still attracts great attention of researchers. Such an interest is explained by the key role of this reaction in sonochemistry. The chemical species ($OH^{\bullet}$, H, H_2O_2, H_2) formed during the ultrasonic treatment of water contribute to advanced oxidation processes of organic pollutants [2,3] and redox reactions of d- and f-transition metal ions in aqueous solutions [4-6]. The strongly endothermic dissociation of H_2O molecule (E_d = 497 kJ·mol^{-1}) provided the first evidence for drastic conditions inside the cavitation bubble. Despite numerous studies, the origin of the extreme conditions produced by cavitation event remains a subject of debate. According to the conventional model of cavitation developed in the 1950s, homolytic bond cleavage of H_2O molecule is triggered by near-adiabatic heating of the intrabubble gas/vapor mixture during bubble collapse [7-9]:

$$H_2O \; -))) \rightarrow H + \; OH^{\bullet} \qquad (1)$$

Further mutual recombination of $OH^{\bullet}$ radicals and H atoms gives H_2O_2 and H_2 respectively. However, the recent finding of nonequilibrium plasma produced in water during multibubble cavitation [10,11] raised a question about the contribution of ionized species to the process of

sonochemical water splitting. Study of the H/D kinetic isotope effect (KIE), or in other words the kinetics of isotopically substituted molecules, is commonly employed to clarify the reaction mechanism [12]. In chemical kinetics, the H/D isotope separation factor α is calculated as $\alpha = (\frac{H_2}{D_2})/(\frac{H_2}{D_2})_0$, where $(\frac{H_2}{D_2})_0$ is the initial isotopic composition and $(\frac{H_2}{D_2})$ is the isotopic composition of the reaction products. With regard to the classical theory, the H/D KIE during H_2O homolytic splitting is determined entirely by zero-point energy difference of the ground states for O-H and O-D bonds (ΔE = 5.80 kJ·mol^{-1}) and the transition states can be neglected [12]: $\alpha = \exp(\Delta E/RT_g)$, where T_g is the gas temperature. Sonoluminescence (SL) spectroscopy of $OH^{\bullet}$ radicals produced by 20 kHz ultrasound in H_2O saturated with argon allowed access to a gas temperature inside the cavitation bubble, which was found to be close to T_g = 5000 K [13]. This value agrees fairly well with T_g obtained for aqueous solutions of volatile organic compounds using sonoluminescence spectra of C_2* radicals [9,14]. For T_g = 5000 K, the classical approximation suggests quite small H/D α value equal to 1.15. On the other hand, water radiolysis involving ionized species exhibits larger H/D KIE reaching α = 2.4-3.5 at room temperature, which was attributed to quantum tunneling phenomenon [15,16].

Alternatively, the H/D KIE during water sonolysis could occur due to the difference of light and heavy water diffusion into the bubble at the rarefaction stage. In H_2O/D_2O mixtures at $[H_2O] < [D_2O]$, the protium mainly presents as HDO molecules because of the fast isotopic equilibrium (2) [17]:

$$H_2O + D_2O \leftrightarrows 2HDO,\ K_{eq} = 4 \qquad (2)$$

Therefore, the H/D α value can be estimated as the ratio of HDO and D_2O translational diffusion coefficients $\alpha = D_{HDO}/D_{D2O}$. At 25°C, the D_{HDO} and D_{D2O} values are equal to 0.234 [18] and 0.211 [19] Å^2·ps^{-1} respectively leading to α=1.11, which is close to KIE value calculated using zero-point energy approach.

These considerations give us an idea on how to probe the mechanism of water sonochemical dissociation using H/D KIE. Mišik et al. reported a study of KIE in argon-saturated H_2O/D_2O (1:1) mixture exposed to 50 kHz ultrasound using EPR spin-trapping technique [20]. However, this method would enable the detection of only the small fraction of formed H/D atoms that escaped from the cavitation bubble interior. In addition, obtained α values vary over a large range

(1.20-1.71) depending on the spin trap due to rapid decay of trap-H adducts and sonochemical instability of studied trap molecules. As a result, calculated T_g values are also widely scattered from 1200 to 3370 K. Generally speaking, the reported EPR study does not allow to distinguish between classical and quantum tunneling mechanism of water sonolysis. In the present work, the H/D KIE was studied in H_2O/D_2O mixtures saturated with Ar or Xe and treated with 20 kHz ultrasound. Gaseous products of sonolysis were analyzed by mass spectrometry. The overall sonochemical activity was monitored by H_2O_2 formation in sonicated water. In our opinion, this research provided experimental evidence for strong contribution of electron tunneling to the mechanism of water sonochemical splitting.

Knowledge about the gas temperature at the final stage of bubble collapse is crucial to understand the origin of KIE. As mentioned previously, for H_2O saturated with Ar and submitted to 20 kHz ultrasound, the T_g value is close to 5000 K. However, data about T_g in D_2O are missing in the literature. Therefore, in the first stage, we studied the SL spectra of D_2O saturated with Ar and Xe. The experimental setups used for SL and sonochemistry studies are shown in Fig. S1 and Fig. S2 of the Supporting Information, respectively. Further details are presented in the Experimental Section. The experimental SL spectra of D_2O are shown in Fig. S3. Similarly to SL spectra of H_2O [10,14], they exhibit OD ($A^2\Sigma^+$-$X^2\Pi$) and OD ($C^2\Sigma^+$-$A^2\Sigma^+$) emission bands as well as a broad continuum ranging from UV to visible spectral range. The much stronger intensity of OD ($C^2\Sigma^+$-$A^2\Sigma^+$) band in the presence of Xe compared to Ar is explained by higher ionization degree of intrabubble plasma for Xe in line with previous SL data for H_2O [10,21]. Gas temperature was determined from OD ($A^2\Sigma^+$-$X^2\Pi$) emission band (Fig. 1) using spectral simulation with Lifbase software, which assumes a similarity of T_g and T_v values typical for plasmas close to thermal equilibrium [22, 23]. In Ar, the T_g value derived from the simulated spectrum in D_2O (Fig. S4a) is very close to that in H_2O (T_g = 5000 K). On the other hand, in the presence of Xe, the OD ($A^2\Sigma^+$-$X^2\Pi$) emission band cannot be successfully fitted by Lifbase simulation (Fig. S4b). A similar phenomenon reported recently for the SL spectra of H_2O/NH_3 solutions [11] and D_2O [21] saturated with Xe has been attributed to the non-Boltzmann overpopulation of the higher vibrational levels of OH/OD ($A^2\Sigma^+$) excited state. Generally, SL study points out close similarity of the intrabubble conditions for H_2O and D_2O in the presence of noble gases. Sonolysis of H_2O/D_2O mixtures causes accumulation of hydrogen peroxide in the liquid phase and emission of H_2, HD, and D_2 isotopic

mixtures into the gas phase for both studied saturating gases, argon and xenon. It is worth mentioning that mass spectrometric analysis revealed the absence of molecular oxygen in the gaseous products for the entire range of studied conditions. Kinetics of hydrogen peroxide formation in H_2O/D_2O mixtures follows zero-order kinetics (Fig. S5) like in neat H_2O [24]. Fig. 2 shows that H_2O_2 overall formation rate $W(H_2O_2)_t$, where $[H_2O_2]_t = [HDO_2] + [D_2O_2] + [H_2O_2]$, is independent from H_2O/D_2O ratio indicating the similarity of the sonochemical activities in H_2O and D_2O in agreement with SL data. In contrast, $W(H_2O_2)_t$ values in Xe are almost 4.7-times larger than in Ar. In the literature, such a big difference was attributed to greater solubility of Xe compared to Ar, which provides larger concentration of active bubbles, and also to higher rovibronic temperatures produced inside collapsing bubbles in the presence of Xe [21]. The sonochemical data agree well with stronger intensity of SL for Xe-saturated water (Fig. S3a,b).

Typical emission profiles of hydrogen isotopes are shown in Supporting Information (Fig. S6). The experimental α values depicted in Fig. 3 point out the enrichment of released hydrogen with light isotope. It is interesting to note that the observed H/D KIE values are much larger than what is calculated assuming a thermal process for T_g = 5000 K (α = 1.15) indicating the non-classical behavior of the sonochemical water splitting. In addition, the α values sharply decrease with increasing H_2O content in H_2O/D_2O mixture reaching a steady-state value close to α = 1.5±0.1, which also cannot be understood in terms of zero-point energy difference. Similarly, abnormally high experimental KIE values cannot be explained by the difference of HDO and D_2O diffusion coefficients.

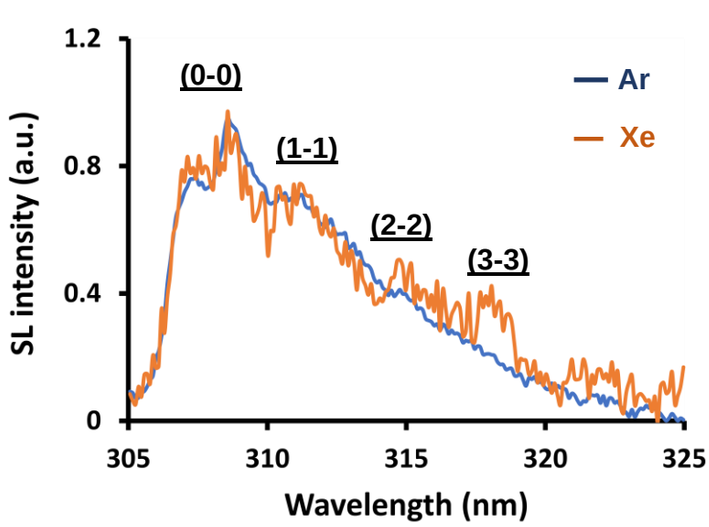

Fig. 1. Experimental OD ($A^2\Sigma^+$-$X^2\Pi$) emission band after subtraction of a baseline and normalization to (0-0) v-v transition. Blue curve is for Ar and orange curve is for Xe. Lifbase simulation is shown in Fig. S4 for Tg = 5000±500 K and P = 500 bar presuming quasi-equilibrium plasma conditions for both systems ($T_v \approx T_g$). The vibrational (v-v) transitions were identified using Lifbase spectral database [22].

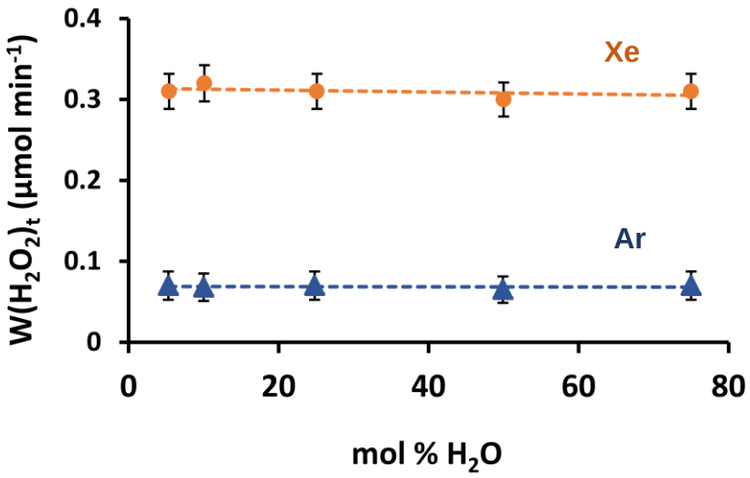

Fig. 2. Variation of hydrogen peroxide formation rate, $W(H_2O_2)_t$, with composition of H_2O/D_2O mixture. f = 20 kHz, P_{ac} = 19 W, T = 20°C.

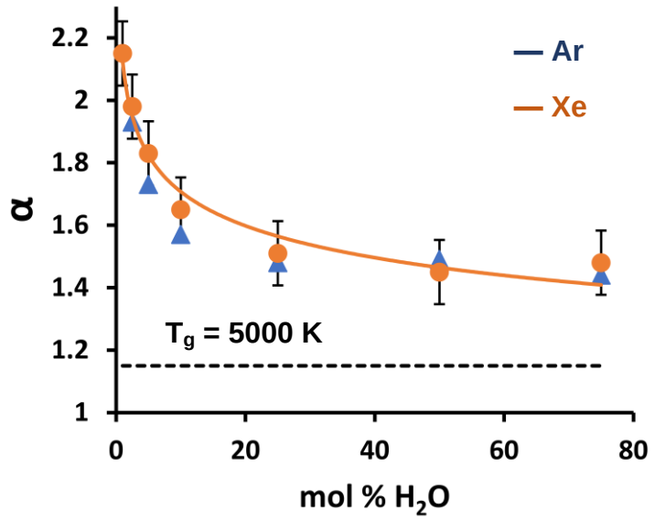

Fig. 3. Dependence of H/D KIE (α) on H_2O concentration in H_2O/D_2O mixtures sparged with Ar (▲) and Xe (●). The dotted line shows calculated α value at T_g = 5000 K presuming classical behavior.

Table 1. Effective gas temperature, T_{eff}, inside the collapsing bubble calculated from experimental H/D KIE factors using classical approach.

H_2O content (mol %)	**Gas**	**α (± 10%)**	**T_{eff} ±120 (K)**
2.6	Ar	1.93	1062
2.6	Xe	1.98	1022
5.3	Ar	1.73	1270
5.4	Xe	1.84	1144
49.9	Ar	1.49	1750
50.0	Xe	1.45	1880

Table 1 summarizes the effective gas temperatures, T_{eff}, inside the bubble calculated using the classical model of KIE for some selected α values acquired at different experimental conditions. One can see that all these temperatures are much lower than T_g = 5000 K measured using sonoluminescence spectra. Moreover, the calculated values of T_{eff} are even lower than the minimum temperature required for thermal dissociation of water molecule, which is estimated from published thermodynamic data as $T_g \approx 2200$ K at P = 1 bar (≤ 3% of all H_2O are dissociated) [25]. It is worth noting that the temperature of H_2O dissociation increases with pressure because of the positive entropy of this reaction. Therefore, according to the classical approximation, sonochemical water splitting should not occur at T_g = 1022 – 1880 K and P ≈ 500 bar (typical pressure at the final stage of bubble collapse) [11,13]. On the basis of the above data, it can be concluded that the model of thermal homolytic water splitting fails to account for the observed H/D KIE. On the other hand, the sonochemical KIE exhibits a striking resemblance with that reported for water radiolysis [15,16]. During the latter process, hydrogen atoms are produced by two distinct mechanisms: (i) dissociation of covalent O-H bond of excited H_2O^* molecule formed by the recombination of electrons and H_2O^+ cations and (ii) isothermal conversion of electrons to hydrogen atoms via quantum tunneling. In D_2O/H_2O mixtures at low H_2O concentration, primary ionization mainly occurs for D_2O molecules. By similarity with radiolysis, the following plasma chemical mechanism of sonochemical water splitting may be invoked:

$$D_2O -))) \rightarrow D_2O^+ + e^- \quad (3)$$

$$D_2O^+ + e^- \rightarrow D_2O^* \rightarrow D + OD^\bullet \quad (4)$$

$$e^- \rightarrow e^-_h \quad (5)$$

$$D_2O^+ + D_2O \rightarrow OD^\bullet + D_3O^+ \quad (6)$$

Inside the collapsing bubble, ionization of D_2O (reaction 3) most probably occurs by electron impact or by collisions with metastable Ar^*_m (Xe^*_m) atoms. Part of electrons undergoes a recombinative decay with D_2O^+ ions (reaction 4). Another part of electrons is trapped by water molecules (D_2O, HDO, H_2O) yielding hydrated electrons e^-_h (reaction 5). The D_2O^+ ions can also react quickly by deuteron transfer to an adjoining D_2O molecule giving D_3O^+ species (reaction 6). Rapid isotopic exchange between HDO molecule formed by the reaction (2) and D_3O^+ cation would yield protium-containing HD_2O^+ species:

$$D_3O^+ + HDO \rightarrow D_2O + HD_2O^+ \quad (7)$$

Finally, H/D atoms are produced by hydrated electron/hydrogen conversion:

$$e^-_h + HD_2O^+ \rightarrow H + D_2O \quad (8)$$

$$e^-_h + D_3O^+ \rightarrow D + D_2O \quad (9)$$

The reaction of $e^-/D_2O^+(HDO^+)$ recombination (equation 4) is limited by diffusion and therefore should not lead to notable KIE. By contrast, the conversion of electrons to hydrogen atoms in aqueous media at near room and low temperature is known to occur by quantum tunneling of hydrogen atoms and electrons with much higher isotopic selectivity [16, 26]. The observation of anomalous KIE allows us to conclude that the quantum tunneling plays an important role in the sonochemical water splitting. At first it sounds surprising that quantum tunneling may influence the sonochemical reaction since this phenomenon is usually observed at low or near room temperature [27]. Indeed, tunneling of hydrogen atom during sonochemical water splitting is an unlikely process, given that the De Broglie wavelength, λ, of H atom calculated as $\lambda = h/(3m_H kT_g)^{1/2}$, [27] where m_H is the mass of hydrogen, and k is the Boltzmann constant, at T_g = 5000 K is equal to 0.15 pm only. However, the λ value of electron at T_g = 5000 K is equal to 1.5 nm, which is much larger than the size of water molecule (0.275 nm), pointing out the principal possibility of electron tunneling in hot sonochemical plasma. Therefore, the origin of observed KIE may be attributed to the ratio of electron tunneling

probabilities, P_t, toward HD_2O^+ and D_3O^+ cations. According to the Wentzel-Kramer-Brillouin equation (10) [28], P_t is exponentially inversely proportional to the potential barrier width, L, and to the square root of the barrier height, V:

$$P_t = exp\left\{\frac{-4\pi L}{h}[2m(V-E)]^{1/2}\right\} \quad (10)$$

where m is the mass of electron, E is the kinetic energy of electron, and h is the Planck constant. Even a small difference in either the L or V values for HD_2O^+ and D_3O^+ species would create large change of P_t and thereby give rise to a KIE. Incidentally, the conclusion about more efficient barrier penetration by electron for lighter hydrogen isotope is supported by the observation of anomalous KIE in H_2O/D_2O mixtures for outer-sphere electron transfer in some metal ion complexes [29]. The decrease of α values with increasing H_2O concentration in H_2O/D_2O mixture (Fig. 3) is consistent with quantum tunneling mechanism. Indeed, slower electron decay in D_2O compared to H_2O [16,30] provides a broader electron spatial distribution causing higher yield of solvated electrons, which contribute to quantum tunneling reaction pathway. It is interesting that the experimental α values are higher than the calculated "zero-point energy" KIE value in the entire range of studied conditions (Fig. 3). This indicates that the thermal process does not play a significant role in sonochemical water splitting despite the high intrabubble temperature. We believe that the reason for such a surprising conclusion is the extremely short lifetime of the sonochemical plasma which may kinetically inhibit thermal dissociation of H_2O molecule. Time-correlated spectroscopy of a single imploding bubble revealed that the flash width of sonoluminescence related to intrabubble plasma in water ranges from 40 to 350 ps [31]. On the other hand, the characteristic time, $t_{1/2}$, of the thermal water splitting in a mixture with Ar calculated by equation (11) for a second order reaction ($H_2O + Ar \rightarrow H + OH^{\bullet} + Ar$) [32] is much larger and equal to about 0.1 μs at T_g = 5000 K and P = 500 bar. As a result, only a tiny fraction of water molecules (<< 0.1%) can dissociate via thermal mechanism during the lifetime of sonochemical plasma.

$$t_{1/2} = RT_g/Pk_1, \text{ where } k_1 = 2.43\ 10^{-10} \exp\left(\frac{-47117}{T_g}\right) \text{ cm}^3\text{molecule}^{-1}\text{s}^{-1} \quad (11)$$

In contrast, the traversal time for electron tunneling in water computed at distances close to λ value of electron at T_g = 5000 K is in the range of 0.1-1 fs [33] allowing the reaction to occur in a picosecond time range.

Counterintuitively, the H/D KIE is independent from the saturating noble gas (Fig. 3) despite its significant influence on the overall sonochemical activity (Fig. 2). Stronger vibrational excitation of the sonochemical plasma in the presence of Xe observed by sonoluminescence spectroscopy clearly points out the difference of rovibronic temperatures for Xe and Ar. Therefore, the very similar α values observed in Ar and Xe cannot be explained in terms of the classical approach suggested exponential dependence of KIE on the gas temperature. In contrast, KIE driven by quantum tunneling is known to be only slightly influenced by temperature [27, 28]. It can therefore be concluded that the independence of sonochemical H/D KIE on studied noble gases complies with the plasma chemical mechanism involving electron quantum tunneling. In summary, the revealed H/D KIE highlights the importance of ionization processes for sonochemistry in line with recent studies of sonoluminescence spectroscopy [34]. In addition, this research demonstrates the possibility to observe quantum tunneling in picosecond plasmas even at high temperature. Such transient plasmas can be produced not only by acoustic cavitation, but also by other processes, like picosecond electric discharge or picosecond laser ablation, which are intensively being investigated. Finally, we would like to emphasize that tunneling control of chemical reactions becomes so important in chemistry that it has recently been labeled "the third reactivity paradigm" next to kinetic and thermodynamic control [35]. In that optic, a recognition of the concept of quantum tunneling mechanism in sonochemistry can provide a deep and detailed understanding of a variety of reactions driven by cavitation that undergo possibly unrecognized yet tunneling.

Experimental Section. SL was studied in a thermostated stainless steel reactor equipped with a flat quartz window for spectroscopic measurements (Fig. S1). Light emission spectra were recorded in the spectral range from 220 up to 360 nm with a SP 2356i Roper Scientific spectrometer (grating 600blz300, slit 90 μm, spectral resolution 0.8 nm, acquisition time 600 s for Ar and 60 s for Xe) and a CCD camera with UV coating cooled by liquid nitrogen. Spectral calibration was performed using a Hg(Ar) pen-ray lamp (LSP035, LOT-Oriel). Each spectrum was averaged over 10 measurements and corrected for background noise and for quantum efficiencies of gratings and CCD. Sonochemical experiments were performed in a thermostated glass made reactor shown in Fig. S2. For both SL and sonochemical experiments, 50 mL of solution was irradiated with 1 cm^2 ultrasonic probe made of Ti-6Al-4V alloy. The piezoelectric

transducer was supplied by a 20 kHz generator (Vibra-Cell VCX 750 W). The probe was immersed reproducibly 3 cm from the bottom of the reaction vessel. The temperature in the reactor during the process was maintained at a steady-state temperature of 10±1°C for SL and 20±1°C for sonochemical experiments. Pure argon or xenon (both O_2 <1 ppm, Air Liquide) were bubbled at a rate of 94 and 43 mL·min^{-1}, respectively for about 30 min before and during the ultrasonic treatment. The specific absorbed acoustic power, P_{ac} = 19±1 W, transmitted to the solution was measured by conventional thermal probe method [24]. The H_2O/D_2O mixtures were prepared by mixing weighted amounts of ultrapure H_2O (18.2 MΩ cm) and D_2O (99.90% D) with a precision better than 0.1%. Hydrogen peroxide concentration in treated solutions was measured by spectrophotometry with Ti(IV) in 0.6 M H_2SO_4 solutions at 410 nm (ε = 626 cm^{-1} M^{-1}) [24]. Formation of H_2, HD, and D_2 species in the outlet gas was monitored with Prima BT Benchtop mass spectrometer (Thermo Scientific). Water vapor in the outlet gas was trapped with 3 Å molecular sieves prior to injection into the mass spectrometric system. The α value was obtained as the ratio $\alpha = (\frac{H_2}{D_2})/(\frac{H_2}{D_2})_0$, where the initial ratio $(\frac{H_2}{D_2})_0$ was equal to the molar composition of H_2O/D_2O mixture, and the experimental $(\frac{H_2}{D_2})$ value was calculated as $\frac{H_2}{D_2} = \frac{I(H_2)+1/2I(HD)}{I(D_2)+1/2I(HD)}$, where I is the mass spectrometric ion intensity of the corresponding hydrogen isotope composition at the steady-state after background subtraction.

References

1. F. O. Schmitt, C. H. Johnson, A. R. Olson, Oxidations promoted by ultrasonic radiation, J. Amer. Chem. Soc. 51 (1929) 370–375.
2. N. N. Mahamuni, Y. G. Adewuyi, Advanced oxidation processes (AOPs) involving ultrasound for wastewater treatment: A review with emphasis on cost estimation, Ultrason. Sonochem. 17 (2010) 990-1003.
3. R. J. Wood, J. Lee, M. J. Bussemaker, A parametric review of sonochemistry: Control and augmentation of sonochemical activity in aqueous solutions, Ultrason. Sonochem. 38 (2017) 351-370.
4. H. Xu, B. W. Zeiger, K. S. Suslick, Sonochemical synthesis of nanomaterials, Chem. Soc. Rev. 42 (2013) 2555-2567.
5. S. I. Nikitenko, L. Venault, R. Pflieger, T. Chave, I. Bisel, P. Moisy, Potential applications of sonochemistry in spent nuclear fuel reprocessing: A short review, Ultrason. Sonochem. 17 (2010) 1033-1040.
6. T. Chave, N. M. Navarro, S. Nitsche, S. I. Nikitenko, Mechanism of Pt(IV) sonochemical reduction in formic acid media and pure water, Chem. Eur. J. 18 (2012) 3879-3885.
7. B. E. Noltingk, E. A. Neppiras, Cavitation produced by ultrasonics, Proc. Phys. Soc. 63B (1950) 674-685.
8. H. Flynn, Cavitation dynamics. Free pulsations and models for cavitation bubbles, J. Acoust. Soc. Amer. 58 (1975) 1160-1170.
9. Y. T. Didenko, W. B. McNamara III, K. S. Suslick, Temperature of multibubble sonoluminescence in water, J. Phys. Chem. A. 103 (1999) 10783-10788.

10. R. Pflieger, H. P. Brau, S. I. Nikitenko, Sonoluminescence from OH($C^2\Sigma^+$) and OH($A^2\Sigma^+$) radicals in water: Evidence for plasma formation during multibubble cavitation, Chem. Eur. J. 16 (2010) 11801-11803.
11. R. Pflieger, T. Ouerhani, T. Belmonte, S. I. Nikitenko, Use of NH($A^3\Pi$-$X^3\Sigma^-$) sonoluminescence for diagnostics of nonequilibrium plasma produced by multibubble cavitation, Phys. Chem. Chem. Phys. 19 (2017) 26272-26279.
12. M. Ceriotti, W. Fang, P. G. Kusalik, R. H. McKenzie, A. Michaelides, M. A. Morales, Markland, Nuclear quantum effects in water and aqueous systems: Experiment, theory, and current challenges, Chem. Rev. 116 (2016) 7529-7550.
13. R. Ji, R. Pflieger, M. Virot, S. I. Nikitenko, Multibubble sonochemistry and sonoluminescence at 100 kHz: The missing link between low- and high-frequency ultrasound. J. Phys. Chem. B. 122 (2018) 6989-6994.
14. R. Pflieger, A. A. Ndiaye, T. Chave, S. I. Nikitenko, Influence of ultrasonic frequency on Swan band sonoluminescence and sonochemical activity in aqueous tert-butyl alcohol solutions, J. Phys. Chem. B. 119 (2015) 284-290.
15. P. Han, D. M. Bartels, H/D Isotope effects in water radiolysis. 2. Dissociation of electronically excited water. J. Phys. Chem. 94 (1990) 5824-5833.
16. H. Muto, K. Matsuura, K. Nunome, Large isotope effect due to quantum tunneling in the conversion reaction of electrons to H and D atoms in irradiated H_2O/D_2O ice, J. Phys. Chem. 96 (1992) 5211-5213.
17. M. Kakiuchi, Distribution of isotopic water molecules, H_2O, HDO, and D_2O, in vapor and liquid phases in pure water and aqueous solution systems, Geochim. Cosmochim. Acta. 64 (2000) 1485-1492.
18. J. Horita, D. R. Cole, Stable isotope partitioning in aqueous and hydrothermal systems to elevated temperatures, in Aqueous systems at elevated temperatures and pressures: Physical chemistry in water, steam and hydrothermal solutions, Ed. D. A. Palmer, R. Fernández-Prini, A. H. Harvey, Elsevier, Amsterdam, 2004.
19. M. Holz, S. R. Heil, A. Sacco, Temperature-dependent self-diffusion coefficients of water and six selected molecular liquids for calibration in accurate 1H NMR PFG measurements, Phys. Chem. Chem. Phys. 2 (2000) 4740-4742.
20. V. Mišik, N. Miyoshi, P. Riez, EPR spin-trapping study of the sonolysis of H_2O/D_2O mixtures: Probing the temperatures of cavitation regions, J. Phys. Chem. 99 (1995) 3605-3611.
21. A. A. Ndiaye, R. Pflieger, B. Siboulet, S. I. Nikitenko, The origin of isotope effects in sonoluminescence spectra of light and heavy water, Angew. Chem. Int. Ed**.** 52 (2013) 2478-2481.
22. J. Luque, D. R. Crosley, LIFBASE: Database and Spectral Simulation, SRI International, Menlo Park, USA, 1999.
23. A. Fridman, Plasma Chemistry, Cambridge University Press, New York, USA, 2008.
24. R. Pflieger, T. Chave, G. Vite, L. Jouve, S. I. Nikitenko, Effect of operational conditions on sonoluminescence and kinetics of H_2O_2 formation during the sonolysis of water in the presence of Ar/O_2 gas mixture, Ultrason. Sonochem. 26 (2015) 169-175.
25. W. T. Parry, J. Bellows, J. S. Gallagher, A. H. Harvey, ASME International Steam Tables for Industrial Use, Second Edition, ASME Press, New York, USA, 2009.
26. S.-I. Ohno, The H/D isotope effect in the conversion of electron into a hydrogen atom in aqueous acid solutions at 300 K and 77 K, Bull. Chem. Soc. Jap. 41 (1968) 1301-1307.
27. R. P. Bell, The Tunnel Effect in Chemistry, Chapman and Hall, New York, USA 1980.
28. J. Meisner, J. Kästner, Atom tunneling in chemistry, Angew. Chem. Int. Ed. 55 (2016) 5400-5413.
29. R. J. Marcus, B. J. Zwolinski, H. Eyring, The electron tunneling hypothesis for electron exchange reactions, J. Phys. Chem. 58 (1954) 432-437.
30. A. C. Chernovitz, C. D. Jonah, Isotopic dependence of recombination kinetics in water, J. Phys. Chem. 92 (1988) 5946-5950.
31. R. A. Hiller, S. J. Putterman, K. R. Weninger, Time-resolved spectra of sonoluminescence, Phys. Rev. Lett. 80 (1998) 1090.
32. N. K. Srinivasan, I. V. Michael, The thermal decomposition of water, Int. J. Chem. Kinet. 38 (2006) 211-219.
33. M. Galperin, A. Nitzan, U. Peskin, Traversal time for electron tunneling in water, J. Chem. Phys. 114 (2001) 9205.
34. S. I. Nikitenko, R. Pflieger, Toward a new paradigm for sonochemistry: short review on nonequilibrium plasma observations by means of MBSL spectroscopy in aqueous solutions, Ultrason. Sonochem. 35 (2017) 623-630.
35. P. R. Schreiner, Tunneling control of chemical reactions: the third reactivity paradigm, J. Am. Chem. Soc. 139 (2017), 15276-15283.